Journal of Magnetism and Magnetic Materials 591 (2024) 171761

Contents lists available at ScienceDirect

Journal of Magnetism and Magnetic Materials

journal homepage: www.elsevier.com/locate/jmmm

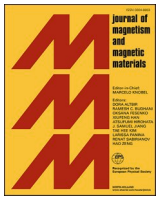

Eigenmodes of 1-kink skyrmions in cylindrical magnetic discs

Trae L. Staggers, Shawn D. Pollard *

Department of Physics and Materials Science, University of Memphis, Memphis, TN 38152, USA

A B S T R A C T

The stability and resonance spectra associated with a domain wall skyrmion embedded within a Néel skyrmion, forming a 1-kink skyrmion, has been studied using micromagnetic simulations. We show that the 1-kink skyrmion is stable over a wide range of fields at moderate strengths of the Dzyaloshinskii-Moriya interaction. By exciting these structures with a broadband magnetic field excitation, we find complex resonance behavior deviating from that of a pure Néel skyrmion. For out-of-plane excitations, the 1-kink skyrmion demonstrates an additional mode relative to that of the Néel skyrmion at reduced amplitude. These consist of low frequency and high frequency modes associated with both a breathing mode and an oscillation of the embedded domain wall skyrmion. Following an in-plane excitation, both Néel and 1-kink skyrmions exhibit a counterclockwise rotational mode with similar frequencies, as well as a higher frequency mode associated with the interaction of the structure with the ferromagnetic background state. These results may help pave the way for exploration of more complex spin structures for magnetic-based microwave devices.

1. Introduction

The study of topological magnetic structures stabilized by the Dzyalloshinskii-Moriya interaction has attracted significant attention in recent years due to their wide range of potential applications, ranging from spin-orbit torque memory and logic devices [1–5] to neuromorphic [6–9] and reservoir computing [10–12]. These objects, including the magnetic skyrmion, are classified by a topological charge,

$$Q = \frac{1}{4\pi}\iint \boldsymbol{m} \bullet \left(\frac{\partial \boldsymbol{m}}{\partial x} \times \frac{\partial \boldsymbol{m}}{\partial y}\right) dxdy$$

where $\boldsymbol{m}$ is the normalized magnetization vector. Skyrmions and other topological objects, such as biskyrmions and merons, are capably of being stabilized down to a few nanometers in extent, efficiently manipulated by spin currents, and, assuming a proper balance of micromagnetic energies, achieve high stability [13–18]. Skyrmions specifically have been shown to exhibit unique dynamics and transport properties such as the skyrmion Hall angle [19–22], topological Hall effect [23,24], and high frequency resonant modes [25–30]. These modes, for an isolated skyrmion, consist of a breathing mode when excited by an out-of-plane excitation, in which the diameter of the skyrmion varies sinusoidally with time, and a counter-clockwise rotational mode when excited with an in-plane excitation, corresponding to counter-clockwise translation of the skyrmion core about a central point [30]. They have been found to vary significantly with externally applied magnetic fields and can be tuned over broad frequency ranges. Because of these interesting resonant modes and their inherent stability, these objects have recently been explored for a variety of applications, including energy harvesting [31] and as magnonic devices [32].

Recently, another object, the domain wall skyrmion, was discovered in magnetic thin films with moderate DMI [33–36]. The domain wall skyrmion describes a winding of the magnetization along the domain wall such that the winding has $Q = \pm 1$. These domain wall skyrmions may be embedded within a traditional magnetic skyrmion, in which case their topological charge adds to the net charge of the skyrmion and is observed as a kink in the skyrmion boundary, and are hence termed n-kink skyrmions, where n- characterizes the total kinks within the system. It was recently demonstrated that, once embedded, these objects can have profound effects on the dynamics of the skyrmion when exposed to spin polarized currents, modifying the skyrmion Hall angle and velocities [37]. However, their influence on resonant dynamics has yet to be explored. In this work, we utilize micromagnetic modelling to determine the influence of a single embedded kink on the resonant dynamics of a 1-kink skyrmion. We find mode splitting and frequency shifts associated with this object, which also observes a significant field dependence. Therefore, these objects may represent a new knob in which to tune resonances in skyrmionics devices. In this paper we explore the resonant modes associated with the insertion of a 1-kink skyrmion with a total topological charge of $Q = -2$.

2. Methods

The system in this work consists of a cylindrical nanodot composed of $256 \times 256 \times 2$ cells with each shell being $0.488 \times 0.488 \times 0.9$ nm^3.

* Corresponding author.
E-mail address: sdpllrd1@memphis.edu (S.D. Pollard).

https://doi.org/10.1016/j.jmmm.2024.171761
Received 1 November 2023; Received in revised form 13 December 2023; Accepted 16 January 2024
Available online 17 January 2024

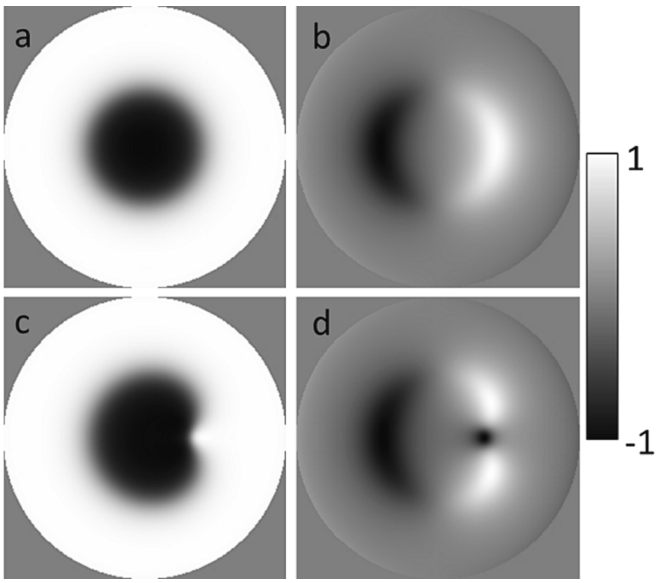

Fig. 1. (a,b) Initial magnetic configuration for a Néel skyrmion showing the normalized z- (a) and x- (b) components of the magnetization, respectively. (c,d) Same as (a,b) but for a 1-kink skyrmion.

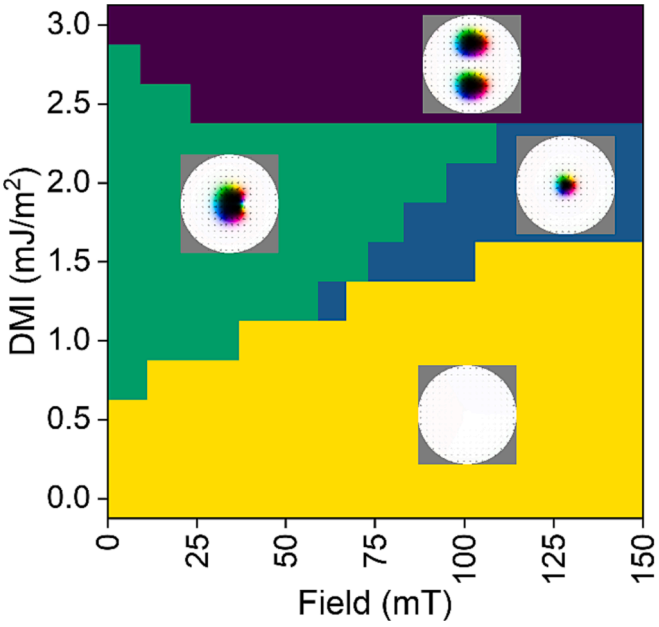

Fig. 2. Phase diagram of an initialized 1-kink skyrmion as a function of DMI strength and magnetic field. The insets show the metastable magnetic configuration corresponding to each region of the diagram.

Micromagnetic modelling was performed utilizing MuMax3 [38,39]. The 1.8 nm total thickness was chosen to enhance the system stability to perturbations. All other parameters were chosen in concordance with ref.[37], with the saturation magnetization $M_S = 1420kA/m$, the exchange stiffness $= 16pJ/m$, the uniaxial anisotropy constant $K_u = 1.36MJ/m^3$, and a damping constant $\alpha = 0.01$. These parameters are consistent with common Pt/Co multilayers [40]. The nanodot was initialized with either a single Néel skyrmion or 1-kink skyrmion at the center, with the core region oriented along the -z direction, and allowed to relax at zero field (Fig. 1). The embedded DW-Sky was chosen to have a net topological charge of Q = -1, adding to the net topological charge of the system, Q_{net}, such that $Q_{net} = -2$. Of note, if opposite DW-Sky topological charge is chosen, $Q_{net} = 0$, which was found to be energetically unstable and would rapidly decay. The interfacial DMI strength was varied to determine the required DMI values and fields in which the 1-kink skyrmion was stable. Subsequent measurements of the resonant modes of the given structures were done at the DMI value determined to give a broad range of field stability while also selecting an experimentally realizable DMI strength D. For this work, this was chosen as 1.5 mJ/m^2. The resonant frequencies were determined by exciting the structure following relaxation by applying a field pulse either parallel or orthogonal to the z-axis and then evaluating the Fourier transform of the magnetization response. The excitation pulse was chosen to be a sinc function with a cut-off frequency of 25 GHz and a delay time of 2 ns. To

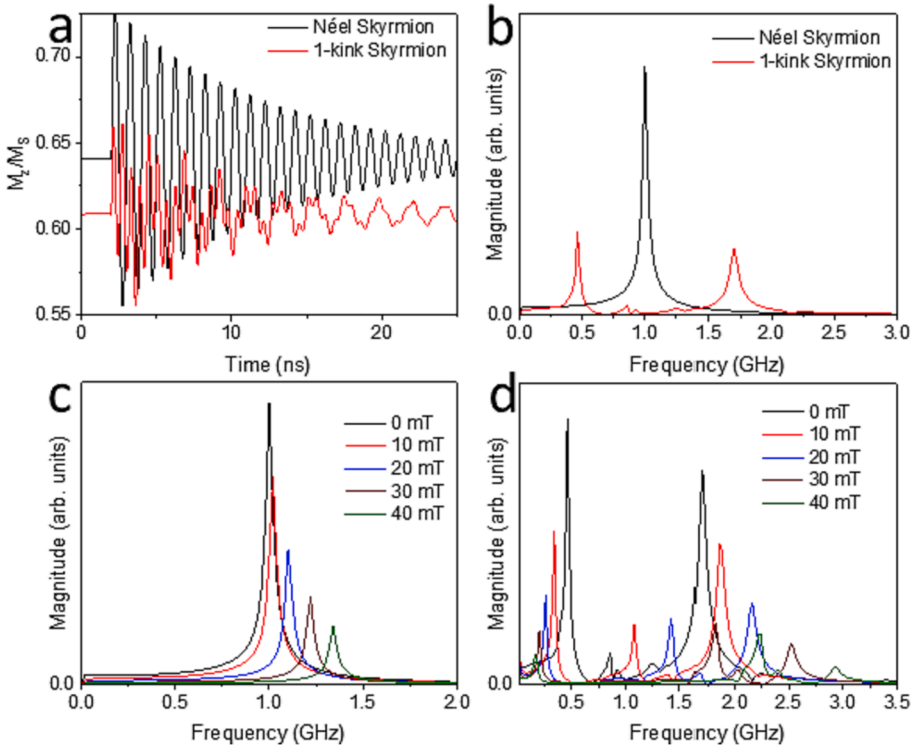

Fig. 3. (a) M_z/M_S versus time for both structures simulated in this work, without any offset field. (b) Frequency spectra taken from the magnitude of the Fourier transform of (a). (c,d) Néel and 1-kink skyrmion resonant spectra for indicated offset fields in the z-direction.

excite a specific mode, a sinusoidal magnetic field with the frequency associated with that mode was applied either in- or out-of-plane, with a magnitude of 1 mT for in-plane excitations and 0.5 mT for out-of-plane. All simulations were performed at a temperature $T = 0K$ and run for 25 ns.

3. Results

The phase diagram in Fig. 2 shows the region of metastability for the system initialized with a 1-kink skyrmion at various values of out-of-plane magnetic field. For values of $D \leq 0.5mJ/m^2$, the system is not stable and decays to the uniform ferromagnetic state. For $0.75mJ/m^2 \leq D \leq 2.75mJ/m^2$, the 1-kink skyrmion is stable over a small field range, which increases to approximately 110 mT at $2.5mJ/m^2$, before decreasing at larger values of D. Of note, at intermediate values of D, the 1-kink skyrmion transforms into a pure Néel skyrmion at increasing fields, while for large D, the system evolves to a two skyrmion state. As $D = 1.5mJ/m^2$ provided a wide range of stability at an experimentally reasonable magnitude, the remainder of this work focuses on this value.

Fig. 3 shows the response of the magnetization for both a Néel skyrmion and 1-kink skyrmion following application of the out-of-plane field pulse. Clear differences are observed in magnetization oscillations as a function of time resulting from the sinc pulse, with the Néel skyrmion exhibiting a single frequency oscillation, with a pair of different frequencies observed for the 1-kink Skyrmion, as demonstrated in Fig. 3a. Note that the z-component of the magnetization is greater for the Néel skyrmion, due to its larger size compared to the 1-kink skyrmion. The distinct frequencies composing the signal are shown in the Fourier transform of the resultant magnetization, shown in Fig. 3b. Of note, there is a very low frequency rotation of the kink location within the kink-skyrmion, with a period, T, of over 50 ns. This drift has been filtered out of the signal using a bandpass filter. The single frequency observed in the Néel skyrmion case splits into multiple distinct modes for the 1-kink skyrmion, with two primary modes, one lower and one higher than in the Néel skyrmion case. The amplitude of each mode is significantly decreased relative to that of the single skyrmion. Fig. 3(c,d) show the effects of an externally applied offset field along the z-axis, aligned to shrink the core region size. For the Néel skyrmion, this results in an increasing resonant frequency as the skyrmion shrinks. However, for the 1-kink skyrmion, the lower frequency mode downshifts in frequency, while the high frequency mode increases. Further, a weak intermediate peak is also observed, which increases in both frequency and magnitude with increasing field. These results were also compared to the case of a uniform ferromagnetic (FM) disc, and no significant resonances were observed below 25 GHz, implying that the observed results are directly related to the presence of the skyrmion states. Of note, no edge modes are observed, which are expected to be present beyond the cut-off frequency used in this work.

Fig. 4 shows the time evolution of skyrmion (Fig. 4a,b) and 1-kink skyrmion (Fig. 4c-f) at frequencies corresponding to resonances in Fig. 3b. For the single skyrmion, the standard breathing mode is observed [28–30]. However, more complex phenomena is observed for the two 1-kink skyrmion modes. The low frequency mode consists of a periodic oscillation of the structure, coincident with a breathing pattern for the entire structure, however, superimposed with an oscillation of the kink itself. The high frequency mode consists of a similar oscillation, including a breathing and oscillating kink. In the high frequency case, the top and bottom hemispheres of the structure, however, oscillate out of phase with each other, and the kink oscillation is much weaker. This emergence of multiple modes is a result of the broken symmetry of the system induced by inclusion of the domain wall skyrmion within the boundary of the Néel skyrmion. This emergence of new modes due to broken symmetry has previously been reported in elliptical disks, wherein symmetry is instead broken by the shape of the disk itself, instead of by embedding defects within the skyrmion boundary [27]. Fig. 5 shows the response of the driven 1-kink skyrmion's intermediate frequency mode at a 40 mT offset. Of note, the breathing mode is largely suppressed, and the oscillation is primarily driven by the oscillatory behavior of the embedded domain wall skyrmion.

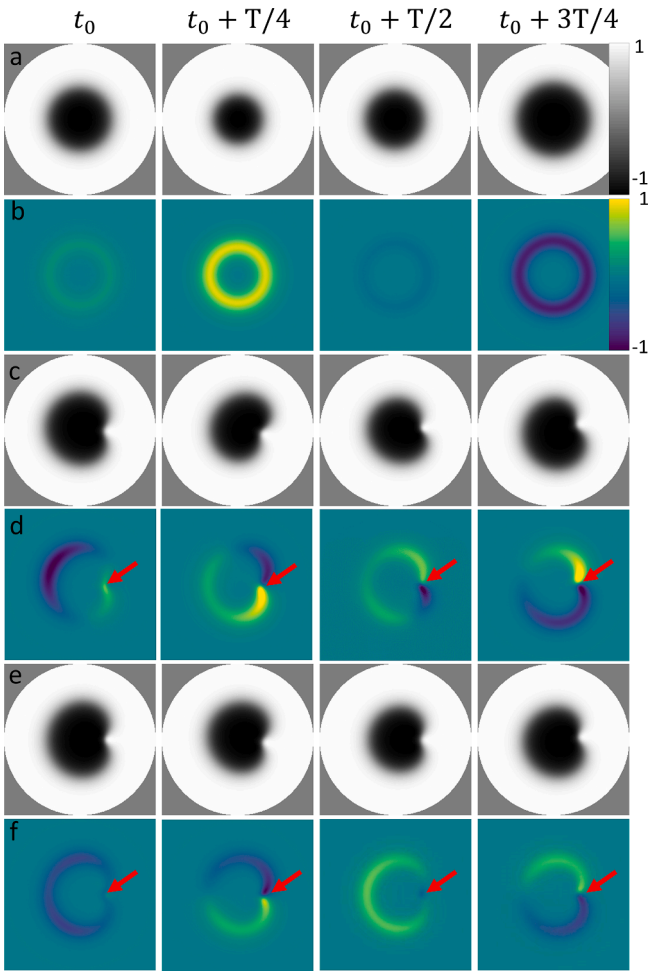

Fig. 4. (a,b) Magnetization state vs. time over a period, T, of the oscillation for an out-plane driven skyrmion at 1000 MHz, showing its out-of-plane breathing mode. (a) shows M_z as a function of time, while (b) shows $[M_z(t) - M_z(0)]/M_S$. (c-f) show the same as (a,b), but at 470 and 1700 MHz, for a 1-kink skyrmion. Each snapshot is taken a quarter of a period from the previous snapshot. The color scale is the same throughout the remaining images in this work. Red arrows indicate the location of the embedded domain wall skyrmion.

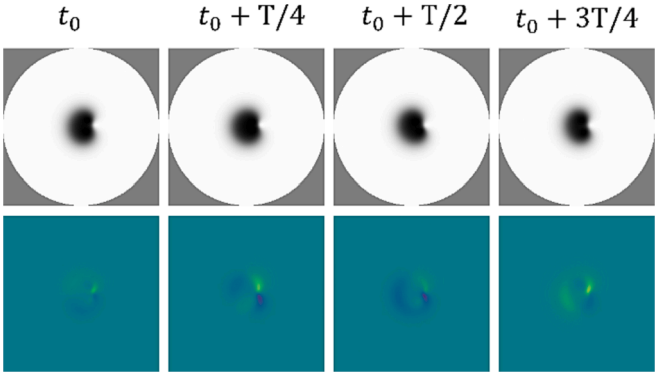

Fig. 5. Magnetization state vs. time over a period, T, of the oscillation for an out-plane driven 1-kink skyrmion at a 40 mT field offset and 2240 MHz (top) and $[M_z(t) - M_z(0)]/M_S$ (bottom).

For an in-plane excitation field, similar time traces of the magnetization are observed. However, in this case, two resonant frequencies are seen in both Néel and 1-kink skyrmion systems (Fig. 6a,b). The complex, weak oscillatory peaks seen in Fig. 6b for the 1-kink skyrmion are artifacts of complex oscillations immediately following excitation, which quickly die out. The effects of an out-of-plane bias field result in a shift of the low frequency mode to higher frequencies, with little change observed in the frequency corresponding to the high frequency mode. These higher frequency modes have been previously described as a result of the precessional motion of the magnetization outside of the skyrmion region, which may also result in a weak dynamics of the core region, and have a significantly weaker dependence on the external field relative to the low frequency mode [25]. In this case here, this corresponds to a very weak counterclockwise rotational mode for the Néel

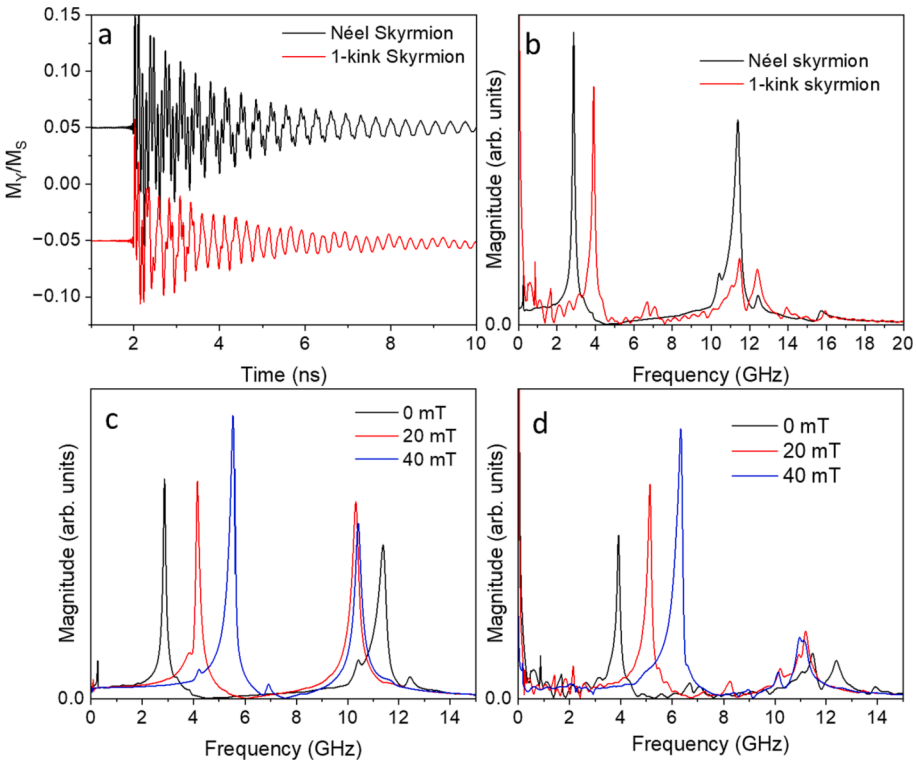

Fig. 6. (a) M_Y/M_S versus time for both structures simulated in this work. (b) Frequency spectra taken from the magnitude of the Fourier transform of (a). (c,d) Effects of an external bias field on the (c) Néel skyrmion spectra and (d) 1-kink skyrmion spectra.

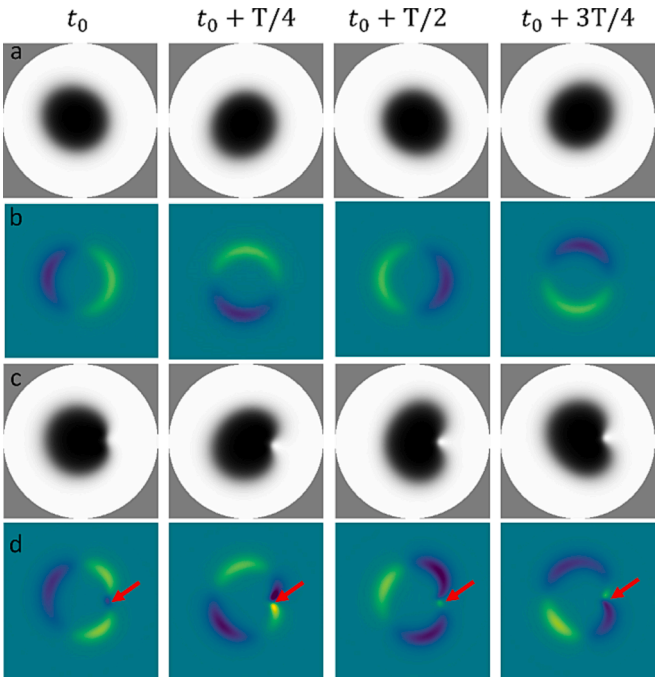

Fig. 7. (a,b) Magnetization state vs. time over a period, T, of the oscillation for an in-plane driven skyrmion at 2860 MHz, showing its counterclockwise rotational mode. (a) shows M_z as a function of time, while (b) shows $[M_z(t) - M_z(0)]/M_S$. (c,d) show the same as (a,b), but at 3920 MHz for a 1-kink skyrmion. Red arrows indicate the location of the embedded domain wall skyrmion.

skyrmion and an even weaker oscillation of the 1-kink skyrmion. The low frequency mode for the Néel skyrmion also describes the well-studied counterclockwise rotational mode, which can be seen in Fig. 7a,b. For the 1-kink skyrmion, the low frequency mode also consists of a clockwise rotation of the embedded domain wall skyrmion and a counter-clockwise oscillation of the kink-skyrmion, shown in Fig. 7c,d, albeit shifted to a higher frequency relative to that for the Néel skyrmion.

4. Summary

To summarize, we have investigated the resonant modes of a single confined 1-kink skyrmion and compared these modes to that obtained for a single isolated Néel skyrmion without the embedded topological charge using micromagnetic modelling. As a result of the broken symmetry introduced by the embedded topological charge, significantly more complex resonant behavior was observed. For an out-of-plane excitation, the primary breathing mode splits into two significantly more complex oscillatory modes, one at lower and one at higher frequency relative to that observed for the Néel skyrmion. For in-plane excitations, the inclusion of the domain wall skyrmion in the Néel skyrmion boundary results in a small shift to a frequency while maintaining the general counterclockwise rotational motion observed without the embedded domain wall skyrmion. As these embedded objects may arise in a variety of films [34,36,41,42], they could provide a means to tune the resonance spectra of skyrmion structures for a variety of applications, but could also pose challenges, leading the emergence of new modes and a decrease in overall amplitude of oscillations. Therefore, to limit the prevalence of kink-type defects, films may be engineered with proper DMI to preclude their stability.

CRediT authorship contribution statement

Trae L. Staggers: Conceptualization, Investigation, Writing – review & editing. **Shawn D. Pollard:** Methodology, Investigation, Resources, Writing – original draft, Supervision.

Declaration of competing interest

The authors declare the following financial interests/personal relationships which may be considered as potential competing interests: [The authors declare the following financial interests/personal relationships which may be considered as potential competing interests: Shawn Pollard reports financial support was provided by National Science Foundation. If there are other authors, they declare that they have no known competing financial interests or personal relationships that could have appeared to influence the work reported in this paper.].

Data availability

Data will be made available on request.

Acknowledgement

Funding from the NSF under grant ECCS-2138271 is gratefully acknowledged.

References

[1] X. Zhang, G.P. Zhao, H. Fangohr, J.P. Liu, W.X. Xia, J. Xia, F.J. Morvan, Skyrmion-skyrmion and skyrmion-edge repulsions in skyrmion-based racetrack memory, Sci Rep. 5 (2015) 7643, https://doi.org/10.1038/srep07643.
[2] Gnoli, L., Riente, F., Vacca, M., Roch, M.R., Graziano, M.: Skyrmion Logic-In-Memory Architecture for Maximum/Minimum Search. Electronics 2021, Vol. 10, Page 155. 10, 155 (2021). Doi: 10.3390/ELECTRONICS10020155.
[3] R. Tomasello, E. Martinez, R. Zivieri, L. Torres, M. Carpentieri, G. Finocchio, A strategy for the design of skyrmion racetrack memories, Sci. Rep. (2014), https://doi.org/10.1038/srep06784.
[4] W. Koshibae, Y. Kaneko, J. Iwasaki, M. Kawasaki, Y. Tokura, N. Nagaosa, Memory functions of magnetic skyrmions, Jpn. J. Appl. Phys. 54 (2015) 053001, https://doi.org/10.7567/JJAP.54.053001/XML.
[5] S. Luo, L. You, Skyrmion devices for memory and logic applications, APL Mater. 9 (2021), https://doi.org/10.1063/5.0042917/43554.
[6] Li, S., Kang, W., Chen, X., Bai, J., Pan, B., Zhang, Y., Zhao, W.: Emerging neuromorphic computing paradigms exploring magnetic skyrmions. In: Proceedings of IEEE Computer Society Annual Symposium on VLSI, ISVLSI. pp. 539–544. IEEE Computer Society (2018).
[7] Song, K.M., Jeong, J.S., Pan, B., Zhang, X., Xia, J., Cha, S., Park, T.E., Kim, K., Finizio, S., Raabe, J., Chang, J., Zhou, Y., Zhao, W., Kang, W., Ju, H., Woo, S.: Skyrmion-based artificial synapses for neuromorphic computing. Nat. Electron. 2020 3:3. 3, 148–155 (2020). Doi: 10.1038/s41928-020-0385-0.
[8] Y. Huang, W. Kang, X. Zhang, Y. Zhou, W. Zhao, Magnetic skyrmion-based synaptic devices, Nanotechnology. 28 (2017) 08LT02, https://doi.org/10.1088/1361-6528/aa5838.
[9] X. Zhang, Y. Zhou, K.M. Song, T.E. Park, J. Xia, M. Ezawa, X. Liu, W. Zhao, G. Zhao, S. Woo, Skyrmion-electronics: writing, deleting, reading and processing magnetic skyrmions toward spintronic applications, J. Phys. Condens. Matter. 32 (2020) 143001, https://doi.org/10.1088/1361-648x/ab5488.
[10] D. Pinna, G. Bourianoff, K. Everschor-Sitte, Reservoir Computing with Random Skyrmion Textures, Phys Rev Appl. 14 (2020) 054020, https://doi.org/10.1103/PhysRevApplied.14.054020.
[11] G. Bourianoff, D. Pinna, M. Sitte, K. Everschor-Sitte, Potential implementation of reservoir computing models based on magnetic skyrmions, AIP Adv. 8 (2018) 055602, https://doi.org/10.1063/1.5006918.
[12] D. Prychynenko, M. Sitte, K. Litzius, B. Krüger, G. Bourianoff, M. Kläui, J. Sinova, K. Everschor-Sitte, Magnetic Skyrmion as a Nonlinear Resistive Element: A Potential Building Block for Reservoir Computing, Phys Rev Appl. 9 (2018) 014034, https://doi.org/10.1103/PhysRevApplied.9.014034.
[13] W. Li, I. Bykova, S. Zhang, G. Yu, R. Tomasello, M. Carpentieri, Y. Liu, Y. Guang, J. Gräfe, M. Weigand, D.M. Burn, G. van der Laan, T. Hesjedal, Z. Yan, J. Feng, C. Wan, J. Wei, X. Wang, X. Zhang, H. Xu, C. Guo, H. Wei, G. Finocchio, X. Han, G. Schütz, Anatomy of Skyrmionic Textures in Magnetic Multilayers, Advanced Materials. 1807683 (2019), https://doi.org/10.1002/adma.201807683.
[14] J. Sampaio, V. Cros, S. Rohart, A. Thiaville, A. Fert, Nucleation, stability and current-induced motion of isolated magnetic skyrmions in nanostructures, Nat Nanotechnol. 8 (2013) 839–844, https://doi.org/10.1038/nnano.2013.210.
[15] Y. Quessab, J.-W. Xu, E. Cogulu, S. Finizio, J. Raabe, A.D. Kent, Zero-Field Nucleation and Fast Motion of Skyrmions Induced by Nanosecond Current Pulses in a Ferrimagnetic Thin Film, Nano Lett. 22 (2022) 6091–6097, https://doi.org/10.1021/acs.nanolett.2c01038.
[16] O. Boulle, J. Vogel, H. Yang, S. Pizzini, D. de Souza Chaves, A. Locatelli, T. O. Menteş, A. Sala, L.D. Buda-Prejbeanu, O. Klein, M. Belmeguenai, Y. Roussigné, A. Stashkevich, S.M. Chérif, L. Aballe, M. Foerster, M. Chshiev, S. Auffret, I. M. Miron, G. Gaudin, Room-temperature chiral magnetic skyrmions in ultrathin magnetic nanostructures, Nat Nanotechnol. 11 (2016) 449–454, https://doi.org/10.1038/nnano.2015.315.
[17] S.D. Pollard, J.A. Garlow, J. Yu, Z. Wang, Y. Zhu, H. Yang, Observation of stable Néel skyrmions in cobalt/palladium multilayers with Lorentz transmission electron microscopy, Nat Commun. 8 (2017) 14761, https://doi.org/10.1038/ncomms14761.
[18] L. Wang, Q. Feng, Y. Kim, R. Kim, K.H. Lee, S.D. Pollard, Y.J. Shin, H. Zhou, W. Peng, D. Lee, W. Meng, H. Yang, J.H. Han, M. Kim, Q. Lu, T.W. Noh, Ferroelectrically tunable magnetic skyrmions in ultrathin oxide heterostructures, Nat Mater. 17 (2018) 1087–1094, https://doi.org/10.1038/s41563-018-0204-4.
[19] S. Woo, K.M. Song, X. Zhang, Y. Zhou, M. Ezawa, S. Finizio, J. Raabe, J.W. Choi, B.-C. Min, H.C. Koo, J. Chang, Current-driven dynamics and inhibition of the skyrmion Hall effect of ferrimagnetic skyrmions in GdFeCo films, Nat Commun. 9 (2018) 959.
[20] W. Jiang, X. Zhang, G. Yu, W. Zhang, M.B. Jungfleisch, J.E. Pearson, O. Heinonen, K.L. Wang, Y. Zhou, A. Hoffmann, S.G.E. te Velthuis, Direct Observation of the Skyrmion Hall Effect, Nat Phys. 13 (2016) 162.
[21] K. Zeissler, S. Finizio, C. Barton, A.J. Huxtable, J. Massey, J. Raabe, A. V. Sadovnikov, S.A. Nikitov, R. Brearton, T. Hesjedal, G. van der Laan, M. C. Rosamond, E.H. Linfield, G. Burnell, C.H. Marrows, Diameter-independent skyrmion Hall angle observed in chiral magnetic multilayers, Nat Commun. 11 (2020) 1–11, https://doi.org/10.1038/s41467-019-14232-9.
[22] K. Litzius, I. Lemesh, B. Krüger, P. Bassirian, L. Caretta, K. Richter, F. Büttner, K. Sato, O.A. Tretiakov, J. Förster, R.M. Reeve, M. Weigand, I. Bykova, H. Stoll, G. Schütz, G.S.D. Beach, M. Kläui, Skyrmion Hall effect revealed by direct time-resolved X-ray microscopy, Nat Phys. 13 (2017) 170–175, https://doi.org/10.1038/nphys4000.
[23] A. Neubauer, C. Pfleiderer, B. Binz, A. Rosch, R. Ritz, P.G. Niklowitz, P. Böni, Topological Hall Effect in the A Phase of MnSi, Phys Rev Lett. 102 (2009) 186602, https://doi.org/10.1103/PhysRevLett.102.186602.
[24] N. Kanazawa, M. Kubota, A. Tsukazaki, Y. Kozuka, K.S. Takahashi, M. Kawasaki, M. Ichikawa, F. Kagawa, Y. Tokura, Discretized topological Hall effect emerging from skyrmions in constricted geometry, Phys Rev b. 91 (2015) 041122, https://doi.org/10.1103/PhysRevB.91.041122.
[25] Satywali, B., Kravchuk, V.P., Pan, L., Raju, M., He, S., Ma, F., Petrović, A.P., Garst, M., Panagopoulos, C.: Microwave resonances of magnetic skyrmions in thin film multilayers. Nature Communications 2021 12:1. 12, 1–8 (2021). https://doi.org/10.1038/s41467-021-22220-1.
[26] S.A. Montoya, S. Couture, J.J. Chess, J.C.T. Lee, N. Kent, M.Y. Im, S.D. Kevan, P. Fischer, B.J. McMorran, S. Roy, V. Lomakin, E.E. Fullerton, Resonant properties

of dipole skyrmions in amorphous Fe/Gd multilayers, Phys Rev b. 95 (2017) 224405, https://doi.org/10.1103/PHYSREVB.95.224405.
[27] Y. Liu, R.K. Lake, J. Zang, Shape dependent resonant modes of skyrmions in magnetic nanodisks, J Magn Magn Mater. 455 (2018) 9–13, https://doi.org/10.1016/J.JMMM.2017.07.007.
[28] V.L. Zhang, C.G. Hou, K. Di, H.S. Lim, S.C. Ng, S.D. Pollard, H. Yang, M.H. Kuok, Eigenmodes of Néel skyrmions in ultrathin magnetic films, AIP Adv. 7 (2017) 055212, https://doi.org/10.1063/1.4983806.
[29] J.V. Kim, F. Garcia-Sanchez, J. Sampaio, C. Moreau-Luchaire, V. Cros, A. Fert, Breathing modes of confined skyrmions in ultrathin magnetic dots, Phys Rev B Condens Matter Mater Phys. 90 (2014) 064410, https://doi.org/10.1103/PHYSREVB.90.064410.
[30] K.Y. Guslienko, Z.V. Gareeva, Magnetic skyrmion low frequency dynamics in thin circular dots, J Magn Magn Mater. 442 (2017) 176–182, https://doi.org/10.1016/J.JMMM.2017.06.094.
[31] G. Finocchio, M. Ricci, R. Tomasello, A. Giordano, M. Lanuzza, V. Puliafito, P. Burrascano, B. Azzerboni, M. Carpentieri, Skyrmion based microwave detectors and harvesting, Appl Phys Lett. 107 (2015) 20, https://doi.org/10.1063/1.4938539/235835.
[32] Z. Chen, F. Ma, Skyrmion based magnonic crystals, J Appl Phys. 130 (2021) 90901, https://doi.org/10.1063/5.0061832/157900.
[33] C. Ross, M. Nitta, Domain-wall skyrmions in chiral magnets, Phys Rev b. 107 (2023) 024422, https://doi.org/10.1103/PhysRevB.107.024422.
[34] R. Cheng, M. Li, A. Sapkota, A. Rai, A. Pokhrel, T. Mewes, C. Mewes, D. Xiao, M. De Graef, V. Sokalski, Magnetic domain wall skyrmions, Phys Rev b. 99 (2019) 184412, https://doi.org/10.1103/PHYSREVB.99.184412.
[35] B.-J. Kim, S.-G. Je, Creation of Domain Wall Skyrmion, The Origin of New Physics: Sae Mulli. 73 (2023) 558–562, https://doi.org/10.3938/NPSM.73.558.
[36] M. Li, A. Rai, A. Pokhrel, A. Sapkota, C. Mewes, T. Mewes, D. Xiao, M. De Graef, V. Sokalski, Magnetic domain wall substructures in Pt/Co/Ni/Ir multi-layers, J Appl Phys. 130 (2021) 153903, https://doi.org/10.1063/5.0056100.
[37] F. Nasr, C.E. Fillion, O. Boulle, H. Béa, L.D. Buda-Prejbeanu, Static and dynamic properties of 1-kink skyrmion in Pt/Co/MgO trilayer, Phys Rev b. 104 (2021) 174441, https://doi.org/10.1103/PHYSREVB.104.174441.
[38] A. Vansteenkiste, J. Leliaert, M. Dvornik, M. Helsen, F. Garcia-Sanchez, B. Van Waeyenberge, The design and verification of MuMax3, AIP Adv. 4 (2014) 107133, https://doi.org/10.1063/1.4899186.
[39] A. Vansteenkiste, B. Van De Wiele, MUMAX: A new high-performance micromagnetic simulation tool, J Magn Magn Mater. 323 (2011) 2585–2591, https://doi.org/10.1016/j.jmmm.2011.05.037.
[40] Boulle, O., Vogel, J., Yang, H., Pizzini, S., De Souza Chaves, D., Locatelli, A., Menteş, T.O., Sala, A., Buda-Prejbeanu, L.D., Klein, O., Belmeguenai, M., Roussigné, Y., Stashkevich, A., Mourad Chérif, S., Aballe, L., Foerster, M., Chshiev, M., Auffret, S., Miron, I.M., Gaudin, G.: Room-temperature chiral magnetic skyrmions in ultrathin magnetic nanostructures. Nature Nanotechnology 2016 11: 5. 11, 449–454 (2016). https://doi.org/10.1038/nnano.2015.315.
[41] J.A. Garlow, S.D. Pollard, M. Beleggia, T. Dutta, H. Yang, Y. Zhu, Quantification of Mixed Bloch-Néel Topological Spin Textures Stabilized by the Dzyaloshinskii-Moriya Interaction in Co / Pd Multilayers, Phys Rev Lett. 122 (2019) 237201, https://doi.org/10.1103/PhysRevLett.122.237201.
[42] J.A. Garlow, M. Beleggia, S.D. Pollard, H. Yang, Y. Zhu, Unconventional domain-wall pairs and interacting Bloch lines in a Dzyaloshinskii-Moriya multilayer thin film, Phys Rev b. 102 (2020) 214429, https://doi.org/10.1103/PHYSREVB.102.214429.